



EUROfusion

EUROFUSION WPMAT-PR(15) 14575

Jan Hoffmann et al.

Improvement of reduced activation 9%Cr steels by Ausforming

Preprint of Paper to be submitted for publication in
Nuclear Materials and Energy



This work has been carried out within the framework of the EUROfusion Consortium and has received funding from the Euratom research and training programme 2014-2018 under grant agreement No 633053. The views and opinions expressed herein do not necessarily reflect those of the European Commission.

This document is intended for publication in the open literature. It is made available on the clear understanding that it may not be further circulated and extracts or references may not be published prior to publication of the original when applicable, or without the consent of the Publications Officer, EUROfusion Programme Management Unit, Culham Science Centre, Abingdon, Oxon, OX14 3DB, UK or e-mail Publications.Officer@euro-fusion.org

Enquiries about Copyright and reproduction should be addressed to the Publications Officer, EUROfusion Programme Management Unit, Culham Science Centre, Abingdon, Oxon, OX14 3DB, UK or e-mail Publications.Officer@euro-fusion.org

The contents of this preprint and all other EUROfusion Preprints, Reports and Conference Papers are available to view online free at <http://www.euro-fusionscipub.org>. This site has full search facilities and e-mail alert options. In the JET specific papers the diagrams contained within the PDFs on this site are hyperlinked

Improvement of reduced activation 9%Cr steels by Ausforming

J. Hoffmann(1), M. Rieth(1), L. Commin(1), P. Fernández(2), M. Roldán(2)

¹*Karlsruhe Institute of Technology (KIT), 76344 Eggenstein-Leopoldshafen, Germany.*

²*National Fusion Laboratory-Fusion Materials, CIEMAT, 28040 Madrid, Spain.*

Abstract

For improved performance of the components in a fusion reactor, an increased application temperature for structural materials such as 9%Cr reduced activation steels is crucial. The improvement of the current generation of 9%Cr steels (i.e. EUROFER) is one of the aims of the current EUROfusion programme for advanced steels. The goal of this work is to determine the most effective thermo-mechanical treatment of reduced activation ferritic martensitic steels with respect to high-temperature strength. Compatibility of these treatments with industrial production processes is essential.

In the present study, two different batches of EUROFER-2 were prepared with a thermo-mechanical treatment. The materials were solution annealed at 1250 °C and then slowly cooled to the rolling temperature, which was varied between 600 and 900 °C. Hot-rolling was performed in the austenite regime with a subsequent rapid cooling to form the ferritic-martensitic structure. The characterization of the materials was done in as-rolled state and after a subsequent tempering at 750 °C.

The materials characterization was performed by tensile and Charpy impact tests using miniaturized specimens. The microstructure was characterized by scanning electron microscopy (SEM) backscatter images and electron backscatter diffraction (EBSD) maps. All the results were compared to those of conventionally processed EUROFER-2 alloys.

The first results show a gain in tensile strength of approximately 50 MPa at temperatures above 600 °C compared to conventionally treated EUROFER alloys. Microstructural investigations reveal a fine and homogeneous distribution of the martensitic laths, while the prior austenite grains are about one order of magnitude larger. This can be explained by the exceptionally high austenitization temperature compared to the as-received state.

This work has been carried out within the framework of the EUROfusion Consortium and has received funding from the Euratom Research and Training Programme 2014–2018 under grant agreement no. 633053. The views and opinions expressed herein do not necessarily reflect those of the European Commission.

Keywords: Fusion, EUROFER, steels, ferritic-martensitic

Introduction

Reduced activation ferritic martensitic (RAFM) 9%Cr steels have been the subject of research within the fusion community for years. These materials are members of a class of Fe-based alloys with varying and carefully balanced amounts of alloying elements such as Cr, W, Ta, and V [1]. They show an improved void swelling even under high irradiation doses [2]. The amount of carbon and nitrogen needs to be adjusted with caution in order to form strengthening secondary phases. The distribution and nature of the carbides and nitrides which form after heat treatments have been well studied [3,4]. However, a possible improvement of the alloys could be achieved by adjusting the chemical composition and distribution of these secondary phases inside the material. In particular, the amount and size of M₂₃C₆-type carbides need to be controlled. Coarsening and agglomeration of this phase can have a detrimental effect on the impact properties [5].

For increased performance of the components in a fusion reactor, an increase of the application temperature for structural materials such as 9%Cr reduced activation steels is crucial. The improvement of the current generation of 9%Cr steels (i.e. EUROFER) is one of the aims of the current EUROfusion programme for advanced steels. The goal of this work is to determine the most effective thermo-mechanical treatment of RAFM steels with respect to high-temperature strength. Compatibility of these treatments with industrial production processes is essential.

High-temperature tensile strength and creep strength are especially important for future applications in a DEMO fusion reactor [6]. All results are compared to those of a conventionally treated EUROFER97/2 plate. The results of this study give direct input regarding the new experimental alloys proposed within EUROfusion.

Materials and methods

Plates of two different EUROFER97-2 batches with a thickness of 25 mm were processed at OCAS, Gent. The chemical compositions of the alloys are given in Table 1. Only minor differences between the two batches exist.

The thermo-mechanical treatment consisted of a solution and austenitization treatment at 1250 °C in air followed by cooling in a second furnace. The temperature of the second furnace was set to the desired rolling temperature (namely 600, 700, 800, and 900 °C). To ensure temperature control during the whole treatment, a dummy plate of the same material was equipped with thermocouples and processed in the same way as the other materials. The temperature was kept constant during the rolling, with reheating if necessary. Prior to any testing and/or microstructural characterization, all materials were annealed at 750 °C for two hours. As-received state refers to EUROFER97/2 materials after treatment at 960 °C for 1.5 hours with quenching in oil followed by 4 hours at 750 °C with air cooling.

Mechanical tests were performed on miniaturized round tensile specimens with a gauge length of 7.6 mm × 2 mm taken out in the rolling direction. The tensile tests were performed between RT and 700 °C under vacuum with a strain rate of $1.6 \cdot 10^{-6} \text{ ms}^{-1}$. KLST-type specimens with a size of 3 × 4 × 27 mm³ were used for the Charpy impact tests. The orientation was LS type with a 1-mm notch. All specimens were cut using electro-discharge machining (EDM).

Microstructural characterizations were mainly done using transmission electron microscopy (TEM, Jeol JEM 3000F) on thin foils in order to determine the effect of the chemical composition and

treatments on the martensite microstructure (packet size, lath size, dislocation density). The precipitate microstructure (nature of precipitates, size distribution) was measured mainly on extraction replicas (including energy filtered TEM, EDX). Bright field and STEM mode with a medium-angle dark field detector (LAADF) were used for imaging.

Electron backscatter diffraction (EBSD) maps were measured on a Zeiss Merlin field emission gun scanning electron microscope (SEM) equipped with an EDAX Hikari high-speed camera operating at 20 kV. The measured data were further processed by OIM Analysis Software v7.2. A step size of 300 μm was used. All data points with a confidence index below 0.1 were discarded. Apart from a Confidence Index Standardization, no cleanup algorithms were performed on the maps.

Results

The tensile tests of the materials showed only minor variations between the different materials (Figure 1). While the material treated at 900 °C shows lower strength at room temperature, in the range of the operation window (550–700 °C) no differences can be observed. The thermo-mechanical treatment (TMT) brought a general increase in strength to the materials. The yield strength is approximately 50 MPa higher than the as-received condition throughout the whole tested temperature range.

The alloys performed worse compared to the as-received condition in the Charpy-impact tests. A shift of the ductile-to-brittle transition temperature (DBTT) to temperatures approximately 30 °C higher can be seen (Figure 2). The as-received condition shows a DBTT of –90 °C. Inhomogeneities and the large prior austenite grain (PAG) sizes in the TMT materials caused a large scatter in the values of the impact energies. Therefore the curves do not show an abrupt drop in energy. The DBTT range was determined to be between –60 and –30 °C.

As expected from the large grain sizes, the creep strength of the steels is greatly enhanced. Figure 3 shows creep curves for the material processed at 700 °C compared to EUROFER97/2 in the as-received condition. The graph shows only a momentary state of the tests since the experiments are still running. Elongations of the TMT alloys are orders of magnitude lower than in the as-received state under the same creep conditions. Since none of the specimens have failed so far, creep-to-rupture times are expected to be greatly prolonged.

The microstructural investigations showed large and elongated primary boundaries (PAGs). Neither of the materials exhibited a full martensitic structure. Despite the annealing at 750 °C for 2 hours, we still observe a high density of dislocations. The TEM images of the different materials show some evidence that the dislocation density drops slightly with increasing rolling temperature. The secondary phases such as MX (X = C,N), M₂X, and M₂₃C₆ carbides and nitrides were not homogeneously distributed. The population of these phases is high in some areas on the martensite lath boundaries and inside the laths. However parts where the density of precipitates is significantly lower were also found.

With increasing rolling temperature, the martensite laths and secondary phases were refined. After rolling at 900 °C we saw a larger amount of fine precipitates (10–20 nm diameter) inside the sub-grains. We also saw a reduction of the particle agglomeration with increasing TMT temperature. Agglomerations of fine MX precipitates were only observed in the materials rolled at 600 °C (Figure 5). Coarse M₂₃C₆ carbides are present in all materials due to the carbon content of 0.1 wt.% (Table

1). Their size and shape were not affected by the rolling conditions. M23C6 particles with a typical sizes range between 100 and 300 nm were measured in all TEM images (Figure 5).

The chemical compositions of the secondary phases were measured by EDS analysis in the TEM. The results are given in Table 2. As mentioned above, M23C6 carbides are present throughout the whole temperature range. The compositions of the other secondary phases are dependent on the rolling temperature. Other carbides and nitrides were measured with varying compositions. Carbides consisted mostly of tantalum and vanadium but other alloying elements such as chromium and tungsten were also detected inside the secondary phases. The materials processed at 800 °C even formed MX-phases with equal amounts of tantalum and vanadium.

While most alloys formed a mix of several different MX carbo-nitrides, only tantalum-carbides and vanadium-nitrides formed in the materials processed at 900 °C. These observations are mostly in compliance with the data from the thermodynamics simulation (Figure 4), which predicts only V-N, Ta-C/N, and M23C6 carbides. No enrichment of iron or other alloying elements like chrome or tungsten is expected in the precipitates. The TMT at 900 °C seems to produce a material with phases near the equilibrium conditions.

The average grain size estimated from SEM and EBSD images is two to three times larger than that of EUROFER97 in the as-received state [7]. In Figure 6, a triple-junction PAG boundary is shown. The adjacent grains can be estimated to be larger than 70 µm at least. The martensite laths are easily visible inside the grains. From the EBSD map, the widths of individual laths can be measured and they are from the low micrometer down to the sub-micron range. The widths differ between PAGs. This can be seen by comparing the middle and lower left grains of Figure 6. Some elongation visible in the image due to the rolling process makes the correct measurement of the actual grain size difficult, but judging from the images in Figure 7, the grain size is 100 µm or more.

Discussion

The higher strength of the materials in the high-temperature regime maybe due to a finer distribution of the secondary phases or an increased dislocation density after TMT and annealing. With the dislocation densities found in the TEM observations, the latter effect is most likely the cause of the increased strength. A behaviour reported by Harries et al. [8], who attribute a gain in tensile high-temperature strength of 50 MPa to a loss of DBTT of -30 °C, could be replicated here.

The carbide and nitride phases found in the TEM have been studied for commercial 9Cr-steels [9] and are in agreement with the predictions from the models. The distribution of the secondary phases along preferred sites has not been reported for conventionally treated EUROFER [3]. Klimenkov et al. found the same correlation for M23C6 at lath and grain boundaries but did not observe this behaviour for TaC. We attribute the location of these particles to the TMT process, where a fine distribution was achieved due to the rolling in the austenite phase. The composition of the nitrides and carbides is similar. The occurrence of only pure M23C6, TaC, and VN after 900 °C TMT can be explained by the higher diffusion rate at this temperature. Therefore an equilibrium state is reached, with those phases being the most favourable ones [10]. Z-phase and Laves phase could not be detected because they only form after long-term high-temperature exposure of the materials [5].

Loss of toughness is reported as a result of either the coarsening of M23C6 particles [11], the tantalum content of the matrix [12], or PAG size. A general conclusion is that increasing the high-

temperature tensile strength leads to a weakening of the toughness [12]. The weaker performance in the Charpy impact tests shown here can be attributed to the large PAGs. PAGs form during the austenitization step of the processing route. A massive increase in PAG size compared to conventional treatments could be observed [13]. Because the materials were held at 1250 °C for 30 minutes, all secondary phases dissolved into the matrix. This is also predicted by the simulation (Figure 4). MX carbides consisting mainly of tantalum and carbon prevent PAGs from growing when using a conventional thermal treatment for EUROFER at 1050 °C [7]. Comparative studies performed by Sandim et al. [14] and Zilnyk et al. [15] showed similar behaviour of the materials.

Similar creep properties in the as-received state (measured in [7,16]) were also found by Mathew et al. [17] for RAFM steels. The values measured in the present work are significantly higher. The authors associate this with the larger PAGs and reduced fast diffusion paths along grain boundaries. Unfortunately, the influence of a different secondary phase distribution cannot be determined yet. The experiments are still running and only TEM images of the as-crept microstructure will be able to clarify this effect.

Conclusions

The thermo-mechanical treatment of EUROFER97/2 leads to a shift in the mechanical and microstructural properties:

From a microstructural point of view, ausforming at 900 °C is the most effective way to refine the microstructure and distribution of the secondary phases. Independently of the rolling temperature, the deformation and treatment of the material lead to an elongated grain structure. In the EUROFER/2 (993391) materials, only MX- and M₂₃C₆-type carbides and nitrides were detected. This is also independent of the TMT temperature.

The high solution treatment at 1250 °C leads to a full dissolution of all carbo-nitrides. This included tantalum-carbides, which cause the prior austenite grain size to grow massively compared to the as-received condition.

A slight increase in tensile strength could be observed even at elevated temperatures. The downside of this increase is the loss in ductility and the increase of the ductile-to-brittle-temperature.

While it was not possible to keep the drop in DBTT small, a major increase in creep strength was observed. As expected, the creep rate was drastically lowered due to the large prior austenite grain size. Finely distributed carbo-nitrides also lead to an improvement. Tests are still running, but the preliminary results look very promising.

Acknowledgements

This work has been carried out within the framework of the EUROfusion Consortium and has received funding from the Euratom Research and Training Programme 2014–2018 and grant agreement no. 633053. The views and opinions expressed herein do not necessarily reflect those of the European Commission. The authors are grateful to all their colleagues at the Karlsruhe Institute of Technology. S. Baumgärtner, B. Dafferner, and M. Hoffmann are especially acknowledged for their contributions. The authors also thank the colleague Dr. Adrián Gómez Herrero from National Centre of Electronic Microscopy for their support and valuable contribution.

Figures

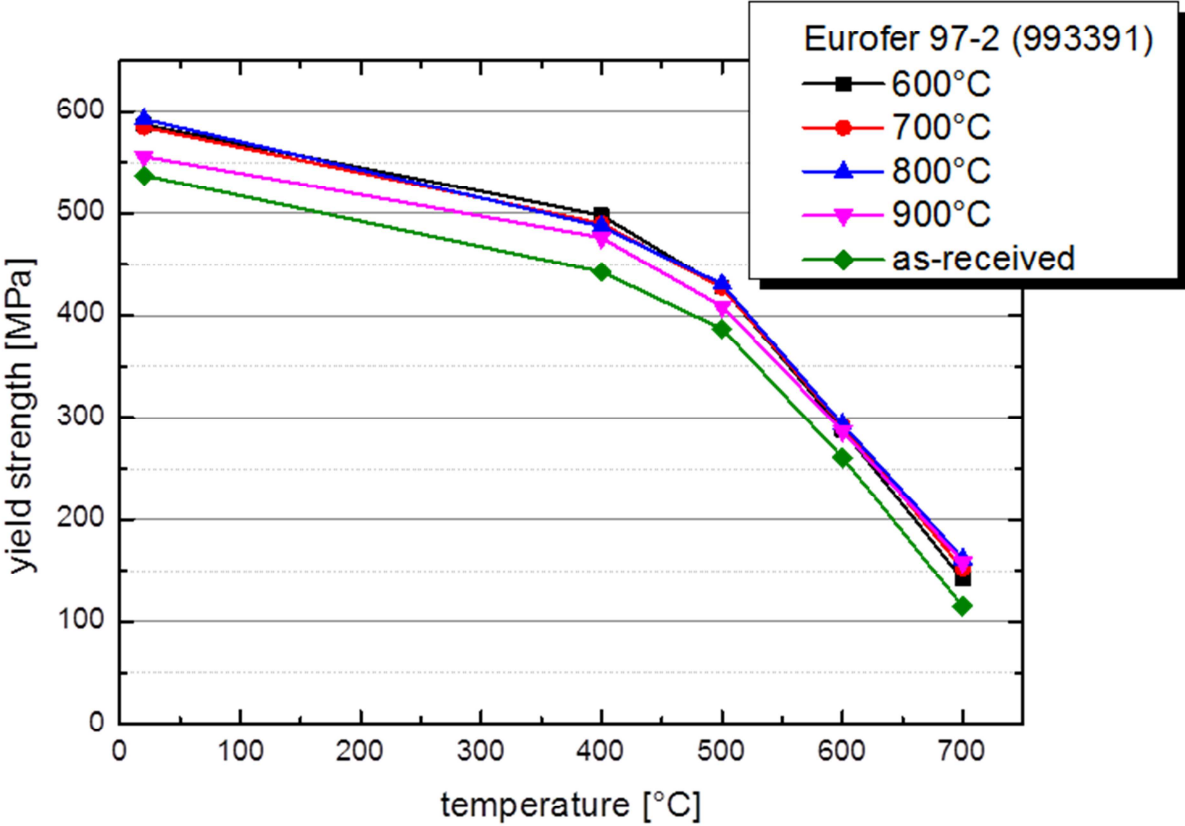


Figure 1 Results of the tensile testing after TMT and in as-received condition (993391)

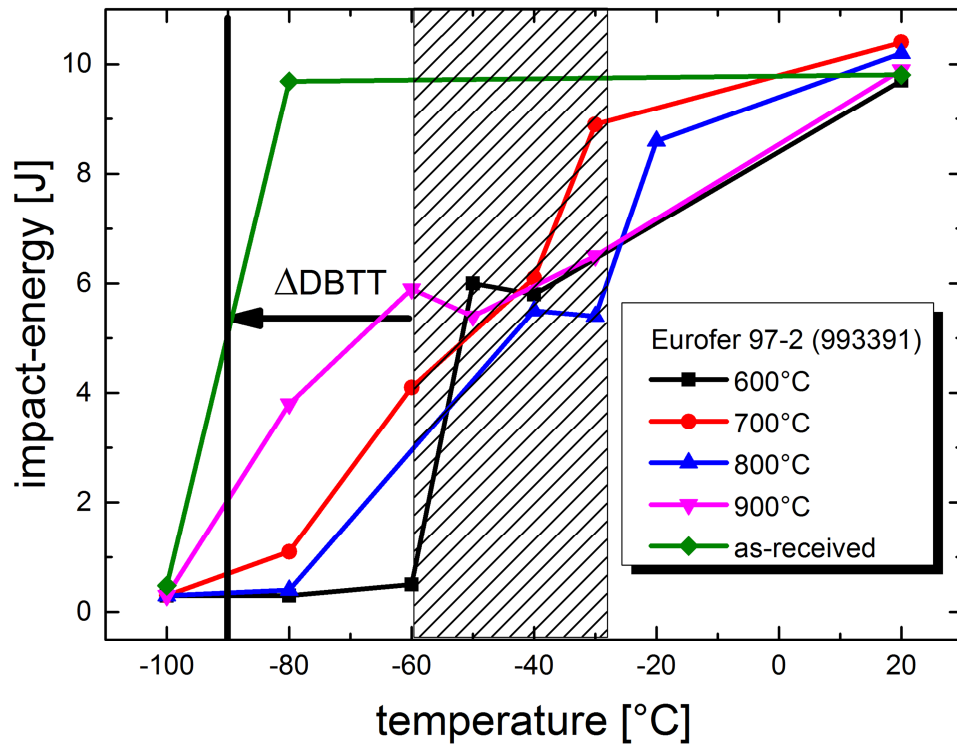


Figure 2 Results of the Charpy impact tests and DBTT shift after TMT and in as-received condition (993391)

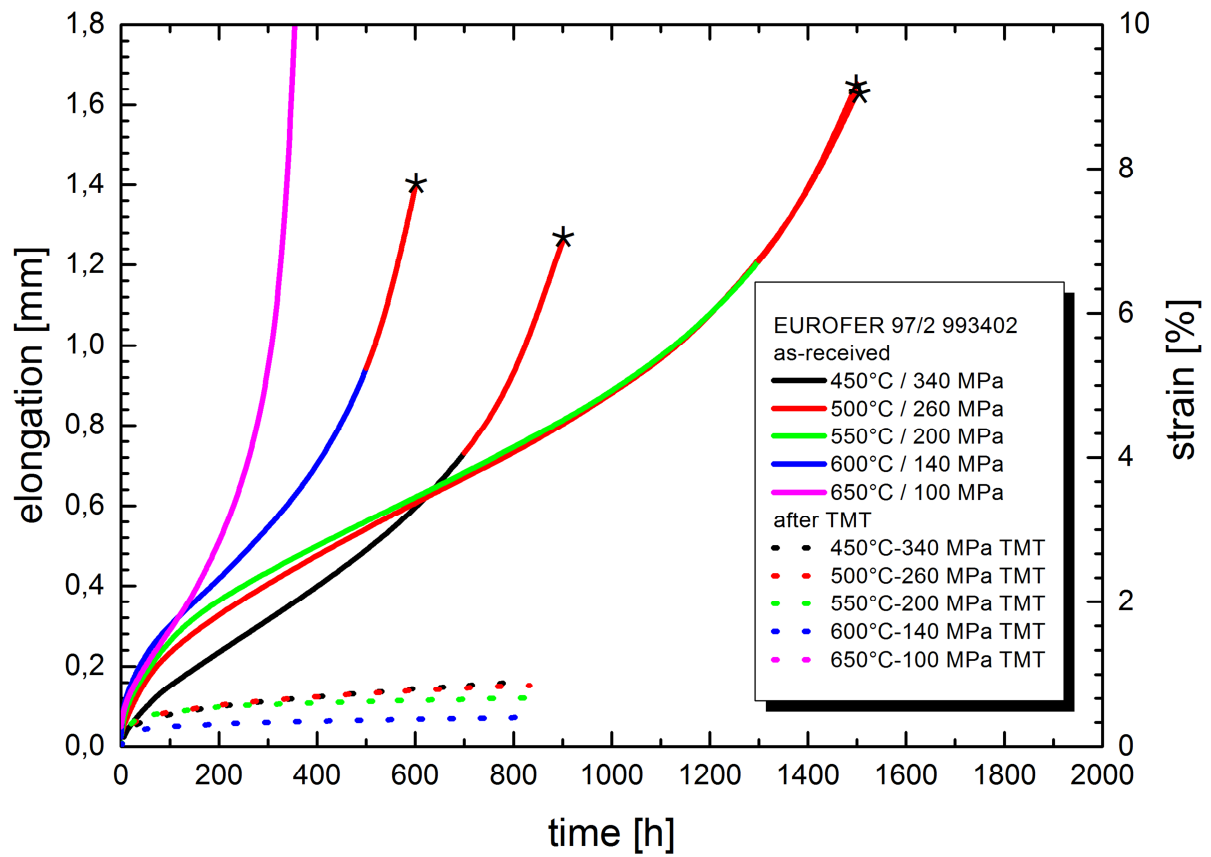


Figure 3 Creep curves of the alloys before and after TMT at 700 °C

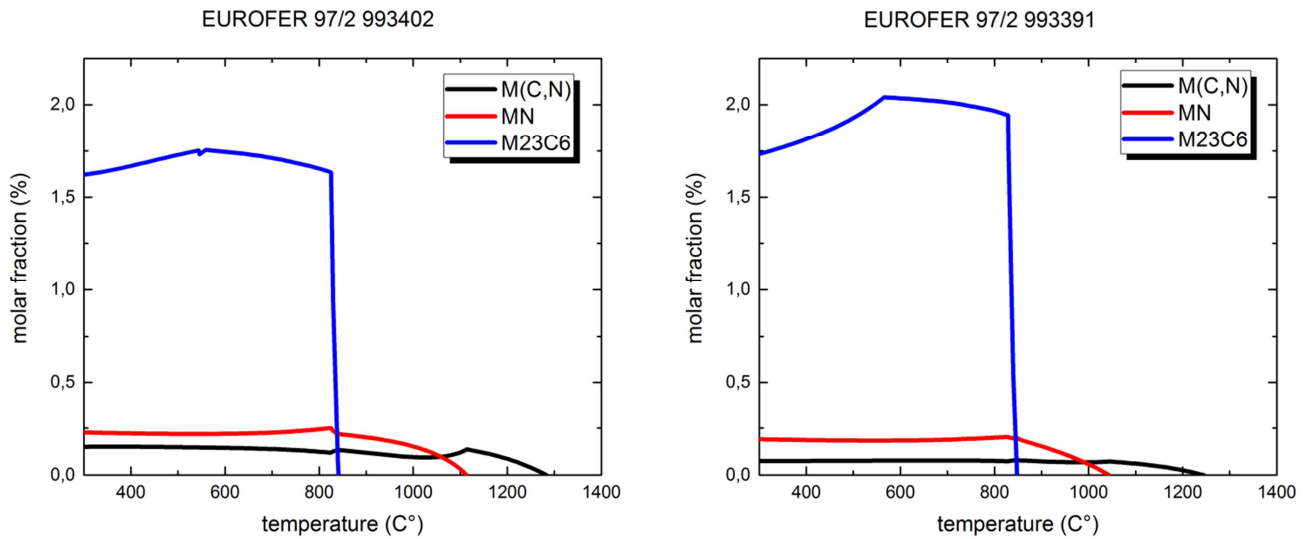


Figure 4 Calculation of the stability of carbide and nitride phases (JMatPro-v5)

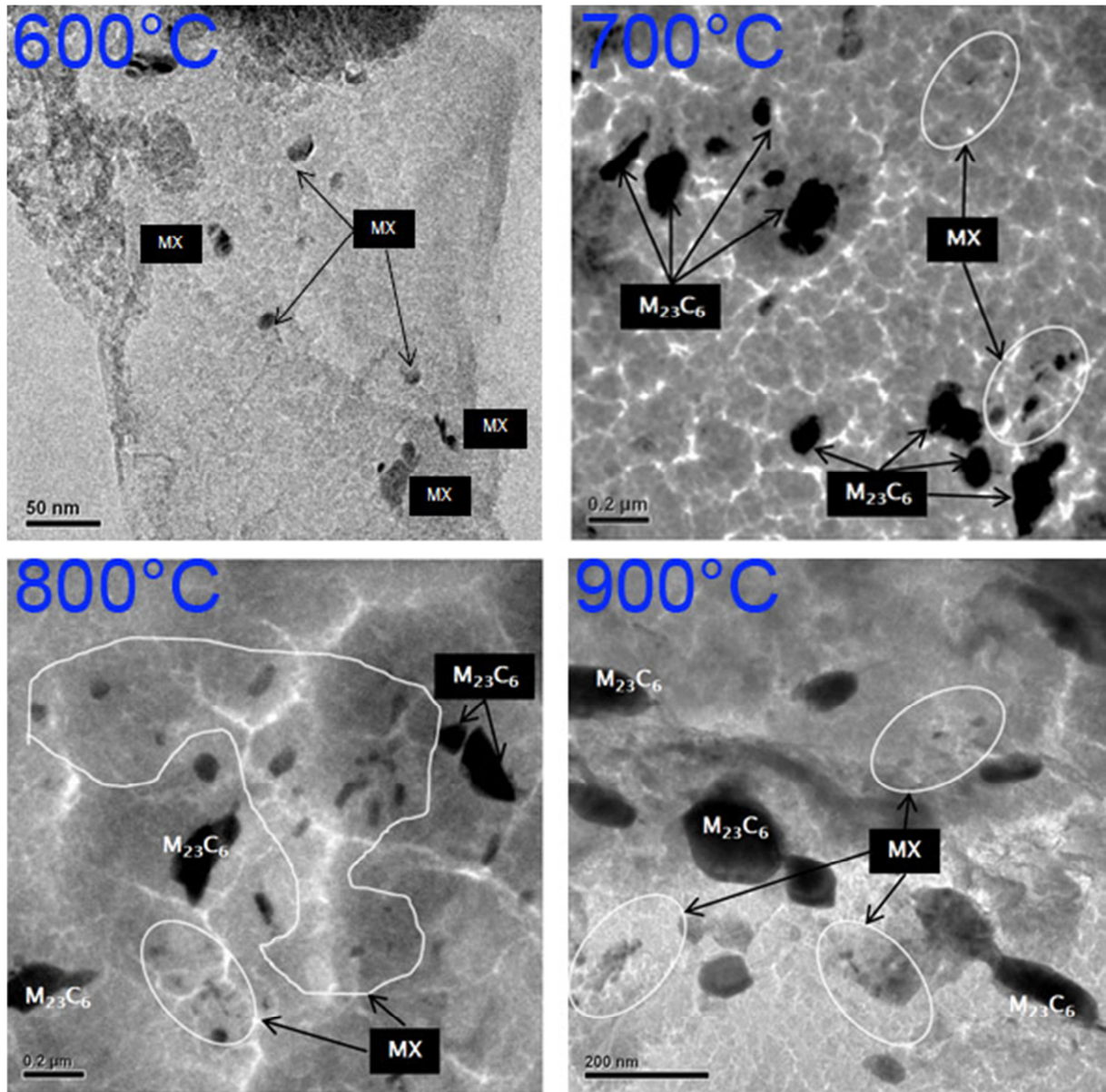


Figure 5 Distribution and composition of precipitates after TMT at different temperatures (993391)

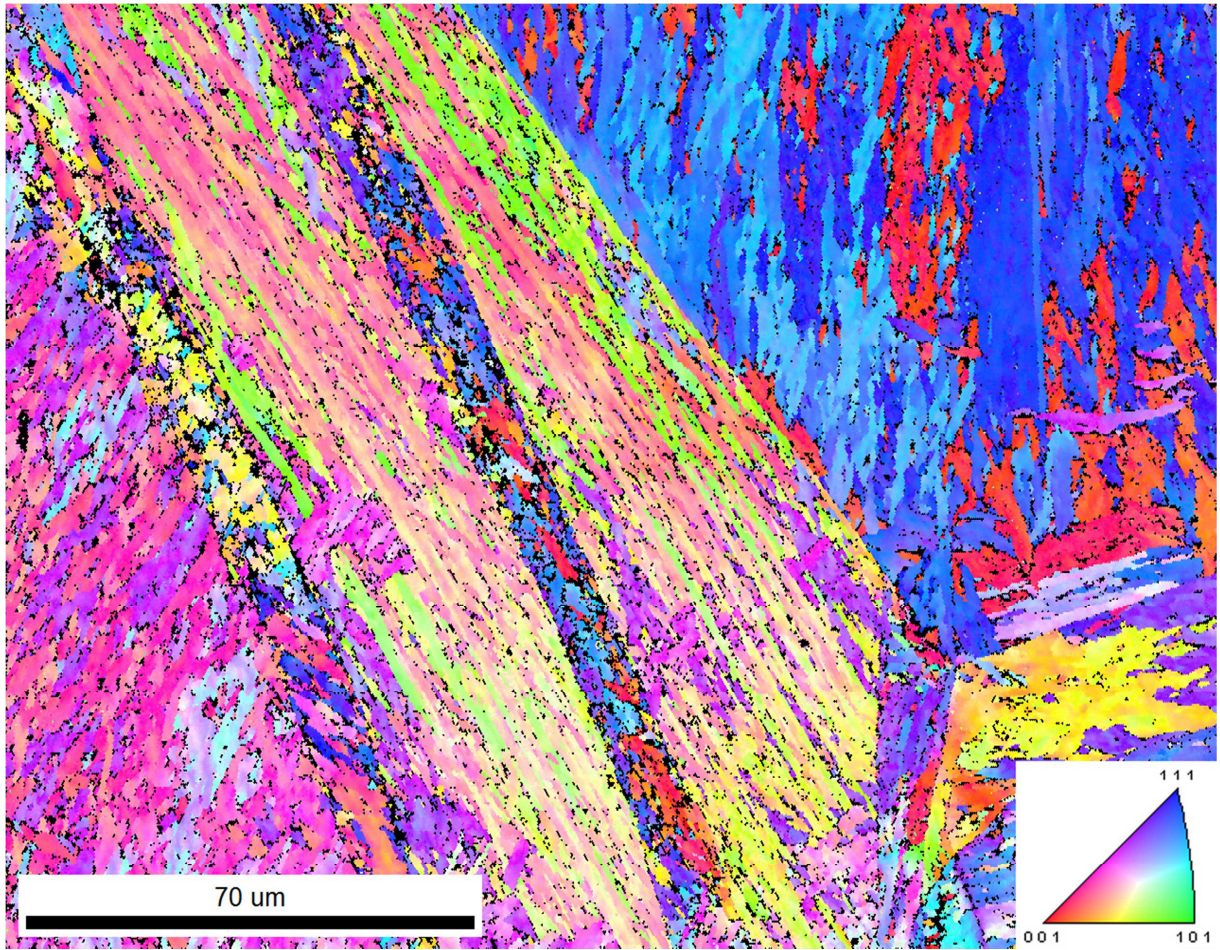


Figure 6 EBSD IPF map of a EUROFER sample, transverse view, calculated along the RD direction (batch 993391, TMT at 800 °C).

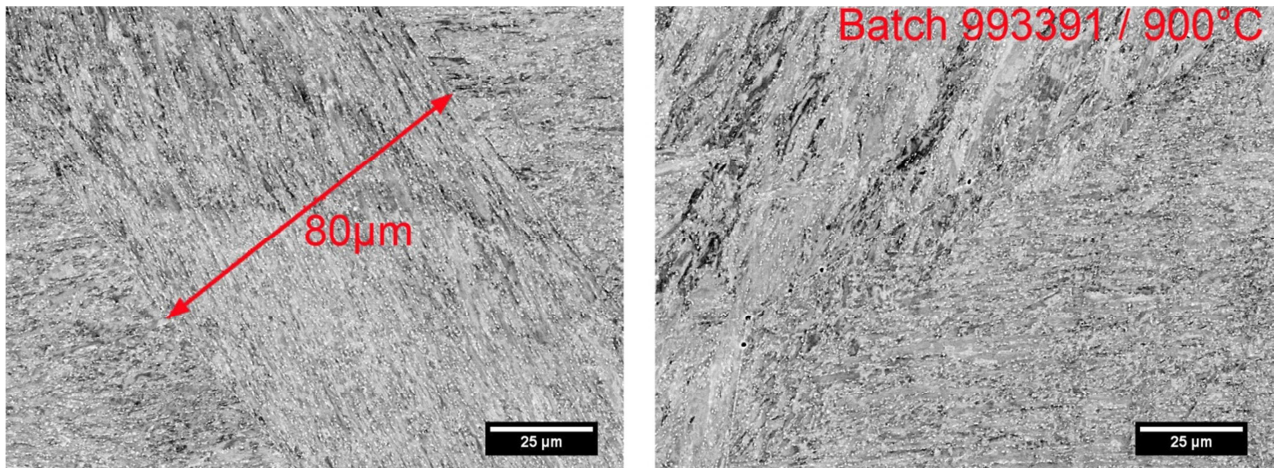


Figure 7 backscatter SEM images showing large prior austenite grains (batch 993391, TMT at 900 °C)

Tables

Batch	W	Cr	V	N	Ta	C	Fe
EUROFER97-2 Batch 993402	1.06	8.9	0.18	0.04	0.15	0.1	balanced
EUROFER97-2 Batch 993391	1.08	8.83	0.2	0.02	0.12	0.1	balanced

Table 1 Chemical composition of EUROFER97-2, all values given in wt.%

600 °C	700 °C	800 °C	900 °C
M ₂₃ C ₆	M ₂₃ C ₆	M ₂₃ C ₆	M ₂₃ C ₆
MX rich in V (Ta, Cr, W, Fe)	MX rich in Ta (V, Cr, Fe)	MX rich in Ta (Ta, V)	MX rich in Ta
MX rich in Ta (Ta, V, Cr, W, Fe)	MX rich in V (Ta, Cr, Fe)	MX rich in V (V, Ta)	MX rich in V
	MX rich in V (Ta, Cr)	MX [Ta]=[V]	
		MX [Ta]= [V]	

Table 2 Chemical composition of secondary phases measured on carbon extraction replicas by TEM

References

- [1] S. Jitsukawa, a. Kimura, a. Kohyama, R.L. Klueh, a. a. Tavassoli, B. Van Der Schaaf, G.R. Odette, J.W. Rensman, M. Victoria, C. Petersen, J. Nucl. Mater. 329-333 (2004) 39–46.
- [2] A. Kohyama, Y. Kohno, K. Asakura, H. Kayano, J. Nucl. Mater. 212-215 (1994) 684–689.
- [3] M. Klimenkov, R. Lindau, E. Materna-Morris, a. Möslang, Prog. Nucl. Energy 57 (2012) 8–13.
- [4] R. Kirana, S. Raju, R. Mythili, S. Saibaba, T. Jayakumar, E. Rajendra Kumar, Steel Res. Int. 86 (2015) 825–840.
- [5] W. Yan, W. Wang, Y.-Y. Shan, K. Yang, Front. Mater. Sci. 7 (2013) 1–27.
- [6] J.F. Salavy, G. Aiello, P. Aubert, L. V. Boccaccini, M. Daichendt, G. De Dinechin, E. Diegele, L.M. Giancarli, R. Lässer, H. Neuberger, Y. Poitevin, Y. Stephan, G. Rampal, E. Rigal, J. Nucl. Mater. 386-388 (2009) 922–926.
- [7] M. Rieth, M. Schirra, A. Falkenstein, P. Graf, S. Heger, H. Kempe, R. Lindau, H. Zimmermann, EUROFER97 Tensile, Charpy, Creep and Structural Tests, Forschungszentrum Karlsruhe GmbH, 2003.
- [8] D.R. Harries, F.B. Pickering, S.R. Keown, Met. Technol. (1977).
- [9] T. Koziel, J. Achiev. Mater. Manuf. Eng. 43 (2010) 200–204.
- [10] W.F. [Hrsg. . Gale, C.J. [Begr. . Smithells, eds., Smithells Metals Reference Book, 8. ed., Elsevier [u.a.], Amsterdam [u.a.], 2004.
- [11] R.L. Klueh, D.R. Harries, High-Chromium Ferritic and Martensitic Steels for Nuclear Applications, 2001.
- [12] L. Schäfer, M. Schirra, K. Ehrlich, J. Nucl. Mater. 237 (1996) 264–269.
- [13] R. Lindau, M. Schirra, Fusion Eng. Des. 58-59 (2001) 781–785.
- [14] M.J.R. Sandim, F.U. Farrão, V.B. Oliveira, E.H. Bredda, a. D. Santos, C. a. M. dos Santos, H.R.Z. Sandim, J. Nucl. Mater. 461 (2015) 265–270.
- [15] K.D. Zilnyk, V.B. Oliveira, H.R.Z. Sandim, a. Möslang, D. Raabe, J. Nucl. Mater. 462 (2015) 360–367.
- [16] a. -a. . Tavassoli, a Alamo, L. Bedel, L. Forest, J.-M. Gentzbittel, J.-W. Rensman, E. Diegele, R. Lindau, M. Schirra, R. Schmitt, H.. Schneider, C. Petersen, a.-M. Lancha, P. Fernandez, G. Filacchioni, M.. Maday, K. Mergia, N. Boukos, P. Spätig, E. Alves, E. Lucon, J. Nucl. Mater. 329-333 (2004) 257–262.
- [17] M.D. Mathew, J. Vanaja, K. Laha, G. Varaprasad Reddy, K.S. Chandravathi, K. Bhanu Sankara Rao, J. Nucl. Mater. 417 (2011) 77–80.